

Conformational behavior of hyaluronan in relation to its physical properties as probed by molecular modeling

Katia Haxaire, Isabelle Braccini, Michel Milas, Marguerite Rinaudo and Serge Pérez¹

Centre de Recherches sur les Macromolécules Végétales, CNRS (associated with Université Joseph Fourier, Grenoble), 38041 Grenoble, France

Received on September 24, 1999; revised on November 9, 1999; accepted on November 14, 1999

Hyaluronan (HA) is a linear charged polysaccharide whose structure is made up of repeating disaccharide units. Apparently conflicting reports have been published about the nature of the helical structure of HA in the solid state. Recent developments in the field of molecular modeling of polysaccharides offer new opportunities to reexamine the structural basis underlying the formation and stabilization of ordered structures and their interactions with counterions. The conformational spaces available and the low energy conformations for the disaccharide, trisaccharide, and tetrasaccharide segments of HA were investigated via molecular mechanics calculations using the MM3 force field. First, the results were used to access the configurational statistics of the corresponding polysaccharide. A disordered chain having a persistence length of 75 Å at 25°C is predicted. Then, the exploration of the stable ordered forms of HA led to numerous helical conformations, both left- and right-handed, having comparable energies. Several of these conformations correspond to the experimentally observed ones and illustrate the versatility of the polysaccharide. The double stranded helical forms have also been explored and theoretical structures have been compared to experimentally derived ones.

Key words: hyaluronan/molecular modeling/helical conformations/persistence length

Introduction

Hyaluronic acid, also called hyaluronan and abbreviated HA, belongs to the family of glycosaminoglycans (GAG). It is made up of repeating disaccharide units of 2-acetamido-2-deoxy- β -D-glucose (GlcNAc) and β -D-glucuronic acid (GlcA) linked 1–4 and 1–3, respectively. HA is the only nonsulfated GAG. The polysaccharide chains are large with average molar masses in the range 10^5 to 10^7 , depending on the source (Laurent, 1970). HA is found in the intercellular matrix of mammalian connective tissues, and it was previously extracted from bovine vitreous humor, rooster combs, and

umbilical cords. It is also produced by some bacteria; for example, it is a significant component of the extracellular material of strains such as *Streptococcus zooepidemicus*, which is used to produce, on a large scale and with a good yield, pure HA having a molar mass around $2\text{--}3 \times 10^6$.

HA participates in a hydrated network with collagen fibers (e.g., vitreous humor), where it acts as an organizing core in the intercellular matrix, connecting together and spatially distributing the cartilage glycoconjugates to form complex intercellular aggregates (Hardingham, 1981; Hascall, 1981). HA is a constituent of the pericellular coat of unfertilized eggs, and a variety of other cells (Goldberg and Tolle, 1984) where it may act in cell–cell interaction and cell adhesion (Underhill and Dorfman, 1978; Mikuni-Takagi and Toole, 1980; Turley and Roth, 1980).

The physical properties and functions of hyaluronan are based on its ability to form viscoelastic aqueous solutions. In solid state, x-ray fiber diffraction has been used in a number of different cationic environments of HA. Left-handed 4-fold helices were found in sodium and potassium environments, and left-handed 3-fold helices with calcium (Sheehan and Atkins, 1983). An extended 2-fold helix has been proposed for the structure of HA under acidic conditions in presence of most cations (Atkins *et al.*, 1972), except potassium and ammonium salts, which form left-handed 4-fold anti-parallel double helices (Sheehan *et al.*, 1977; Arnott *et al.*, 1983). Despite such architectural diversity, all these structures are consistent with the occurrence of intramolecular hydrogen bonds across the glycosidic linkages (Winter and Smith, 1975), and supported by preliminary computer simulations (Scott *et al.*, 1991). In order to get further insight into the hydration features of HA, molecular dynamics simulations have been performed on its constituent disaccharides (Almond *et al.*, 1997) and trisaccharides (Kaufmann *et al.*, 1998). Detailed NMR study of the conformation of one constituting disaccharide has been performed in water (Sicinska *et al.*, 1993). While these investigations are yielding a detailed description of the dynamics of HA oligomers with the surrounding water molecules, they do not offer any comprehensive understanding of the molecular basis which may underline the occurrence of the numerous polymorphs that have been observed for HA.

The purpose of the present study is to further develop our understanding of the physical properties of HA by a detailed exploration of the structural behavior; the work reported here provides, via a series of molecular modeling investigations, a consistent view of the different levels of structural organization and polymorphism that HA can assume. This covers (1) the characterization of the low energy conformers of each constituent di-, tri-, and tetrasaccharide, (2) the dimensions of

¹To whom correspondence should be addressed

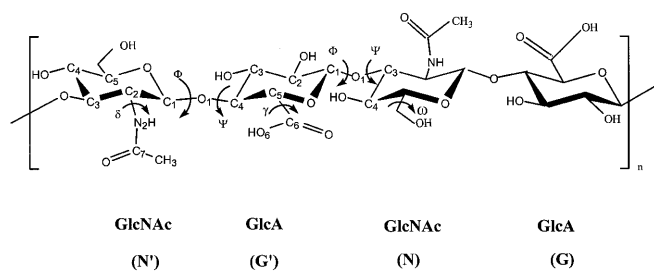


Fig. 1. Schematic representation of the tetrasaccharide β -D-GlcNAc(1 \rightarrow 3) β -D-GlcA(1 \rightarrow 4) β -D-GlcNAc(1 \rightarrow 4) β -D-GlcA, considered as repeat fragment of HA. The GlcNAc residue is abbreviated to as N, whereas the GlcA residue is abbreviated to as G. The labeling of the main atomic positions is indicated, along with the torsion angles of interest.

the polymer in the disordered state (characteristic ratio, persistence length), (3) all the helical conformations, either single and double, that are likely to occur in the solid state, (4) their interaction with essential cations.

Nomenclature

A representation of the tetrasaccharide subunit of HA is given in Figure 1 along with the labeling of the atoms and the torsion angles of interest. For the sake of simplicity and in accordance with previous works, the 2-acetamido-2-deoxy- β -D-glucose (GlcNAc) is abbreviated to as (N), whereas the β -D-glucuronic acid (GlcA) is abbreviated to as (G). All these residues are on their pyranosic form. The conformations around the glycosidic linkages are described by two sets of torsion angles: $\Phi_{1-4} = \text{O5(N)-C1(N)-O1(N)-C4(G)}$, $\Psi_{1-4} = \text{C1(N)-O1(N)-C4(G)-C5(G)}$ [N-G linkage] and $\Phi_{1-3} = \text{O5(G)-C1(G)-O1(G)-C3(N)}$, $\Psi_{1-3} = \text{C1(G)-O1(G)-C3(N)-C4(N)}$ [G-N linkage].

Three other important torsion angles are considered in the study and are those describing the orientation of the following. The acidic group of (G): $\gamma = \text{O5(G)-C5(G)-C6(G)-O6(G)}$. The hydroxymethyl group of (N): $\omega = \text{O5(N)-C5(N)-C6(N)-O6(N)}$. The acetamido group of (N): $\delta = \text{C1(N)-C2(N)-N2(N)-C7(N)}$.

The signs of the torsion angles are in agreement with the IUPAC-IUB commission of Biochemical Nomenclature (IUPAC-IUB, 1983).

Computational methods

Molecular mechanics calculations

The general molecular mechanics program MM3(92) (Allinger *et al.*, 1989, 1990, 1992) was used in this study to compute the energy of any di- or oligosaccharide conformation. The MM3 force field is highly elaborated and includes cross term effects along with the classical bonded and nonbonded terms. This force field is well adapted for the conformational study of carbohydrates (French *et al.*, 1990) and has earned the reputation to be the most appropriate one for this class of biomolecules (in vacuum). It takes into account the anomeric and exo-anomeric effects, and uses an explicit term for hydrogen bonds. The 1992 version includes an angular dependence in the hydrogen bonding function.

Grid search

The available conformational space of the polysaccharides depends mainly on the glycosidic Φ and Ψ torsion angles and can, to a first approximation, be described by the potential energy surface of the disaccharide subunits. Following this assumption, adiabatic maps were computed for β -D-GlcNAc(1 \rightarrow 4)- β -D-GlcA (N-G) and β -D-GlcA(1 \rightarrow 3)- β -D-GlcNAc (G-N) disaccharides. They were constructed from 12 individual relaxed maps computed with starting geometries which take into account the privileged orientations of the hydroxymethyl group (ω close to 60° , -60° , and 180°) and of the secondary hydroxyl groups (clockwise (c) and counter-clockwise (r) orientations). The acidic and N-acetyl groups were positioned in their preferred orientation in all the calculations. This corresponds to the *trans* orientation for the acetamido group and a torsion angle of $\pm 130^\circ$ for the acidic group. In the computation of a relaxed map, the (Φ , Ψ) torsion angles are rotated in 10° increment over the whole angular range, and the resulting conformations are relaxed (with the exception of Φ and Ψ) using the block diagonal method with a termination criterion of $n * 0.00003$ kcal/mol (n : number of atoms).

In order to evaluate long range effects along the chain and the possible occurrence of an inter-residue hydrogen bond network, trisaccharides and tetrasaccharides were built using the results of the preceding conformational study. The conformations of all the local minima of the potential energy surface of N-G and G-N were combined to build the trisaccharides N-G-N and G-N-G, and the resulting geometries were minimized. Finally, a relaxed map was computed for the central N-G and G-N glycosidic linkages of the G-N-G-N and N-G-N-G tetrasaccharides, respectively. In these calculations, the best conformation established for the disaccharides G-N and N-G was applied about the outer glycosidic linkages of G-N-G-N and N-G-N-G, respectively. The isoenergy contour maps were drawn using the program XFarbe.

Generation of statistical chains

In order to evaluate the behavior and the dimensions of HA polymer chains in solution, in θ -conditions, large samples of disordered chains were generated using the Monte Carlo technique as implemented in the METROPOL program (Boutherin *et al.*, 1997). The conformations were selected using the Metropolis algorithm (Metropolis *et al.*, 1953) and distributed according to Boltzmann statistics. The detailed description of the procedure is reported elsewhere (Boutherin *et al.*, 1997). In these calculations, the polymer chain is constructed residue by residue and the program uses the (E, Φ , Ψ) triads describing the conformation about the glycosidic linkages. The usual approach uses the results of the adiabatic map established for the disaccharide subunits and therefore does not take into account all the steric interactions between residues in a longer segment. In order to consider such effects, polymer chains of HA were generated using the (E, Φ , Ψ) triads referring to the relaxed maps of the tetrasaccharide fragments (see above), in addition to the standard procedure. Statistical samples of 20,000 polymer chains each containing 2000 glycosyl residues were constructed for HA (mean error deviation not exceeding 5%). The dielectric constant was set to 80 to simulate aqueous medium, and the following temperatures, 298 K, 323 K, 348 K, and 373 K, were used.

The extension and relative stiffness of the chain are described by the characteristic ratio (C_∞) and the persistence length (L_p) (Lapasin and Pricl, 1995). The average dimensions (C_∞ and L_p) were evaluated from the statistical samples as follows:

$$C_\infty = \lim_{x \rightarrow \infty} C_x = \lim_{x \rightarrow \infty} \langle r^2(x)/x \cdot L_0^2 \rangle \text{ with } r(x) = d(O1(N)-O1(N)[x])$$

The angular brackets indicate the average of the square end-to-end distance r^2 over all the conformations of polymer chains, L_0 is the bond length connecting two adjacent glycosidic oxygen atoms, and x is the number of glycosyl residues. The persistence length (L_p) is defined as the projection of the end-to-end distance vector r on the first bond of the chain. It represents the maximum contour length over which a correlation between monomeric units persists. The asymptotic values of C_x and $L_p(x)$ when x increases, corresponding to a range of x where they become independent of the degree of polymerization (here $x > 500$), i.e., C_∞ and L_p , can be directly compared to the experimental parameters in θ -conditions.

Generation of regular helices

All the possible stable single regular helical forms of HA were established using the program POLYS (Engelsen *et al.*, 1996). The helices are characterized by the two helical parameters n and h , where n is the number of repeat units (disaccharide unit) per turn of the helix and h is the projection of one repeat unit on the helical axis. The chirality of the helix is described by a sign attributed to n : a positive value of n corresponds to a right-handed helix and a negative value to a left-handed helix. The different single helical forms were extrapolated from the low energy conformations of the constitutive G-N and N-G subunits. In the POLYS procedure, two sets of (Φ , Ψ) values, correlated to the local minima for G-N and N-G, are applied on the corresponding (1 \rightarrow 3), (1 \rightarrow 4) glycosidic linkages of the polymer chain, and then, POLYS slightly modifies these values in order to obtain the nearest integral n -fold helical structure. The regular helices are then constructed using the optimized (Φ , Ψ) values. Taking into account the results obtained for the trisaccharides regarding the stability of the conformers, all the reasonable combinations of the low energy conformations of the dimer subunits were explored. Finally, all the optimized single helical structures were minimized (with $\epsilon = 4$ to simulate the solid state) with a constraint applied on the glycosidic linkages in order to preserve the regular helicity.

Under particular conditions, i.e., pH 3–4 and K^+ salt form, HA has been reported to adopt a double helix conformation with anti-parallel strands (Arnott *et al.*, 1983). The occurrence of such a double helix for K^+ -hyaluronate has been debated and several models have been proposed and questioned. In the present study, the feasibility of an anti-parallel double helix for HA was explored using an extension of a home made program CHACHA, originally developed to evaluate the chain-chain interactions (Pérez *et al.*, 1990) and predict crystal structures (Pérez, 1990). In the procedure used, two identical single helices are superimposed along their Z-axis. One helix, chain A, remains unchanged along the procedure. Firstly, chain B, is reversed along Z (rotation 180° around Y-axis). Then, it is rotated over all the angular range around Z (μ : 0° to 360° by 10° intervals) and translated over an integral h length (ΔZ : 0 to 8.2, by 0.818 Å intervals). All the combinations of μ and ΔZ

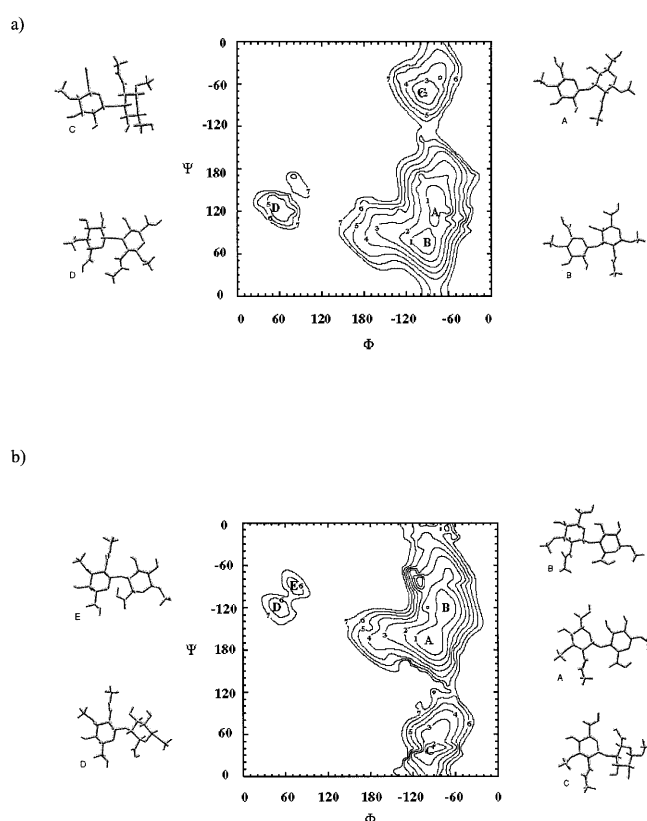


Fig. 2. Adiabatic maps of (a) β -D-GlcA(1-3) β -D-GlcNAc (G-N) and (b) β -D-GlcNAc(1-4) β -D-GlcA (N-G) disaccharides [MM3(92), $\epsilon = 80$] with the energetic wells labeled A, B, C, and D. Contours are drawn in 1 kcal/mol intervals starting from the global minimum. Representation of the low energy conformers in each well are shown.

were explored and for each geometry, the Van der Waals energy was computed. The best conformations were finally relaxed with a constraint applied on the glycosidic linkages. As the number of atoms in the generated double helices is too high for a MM3 minimization, TRIPOS force field with additional PIM parameters (Imberty *et al.*, 1991) were used.

Results and discussion

Conformational properties of the constituent oligosaccharides

The (Φ , Ψ) adiabatic maps of the two disaccharide model fragments, G-N and N-G of HA, computed with a dielectric constant of 80, are displayed in Figure 2. These maps share some common features typical of (1 \rightarrow 3) di-equatorial and (1 \rightarrow 4) di-equatorial linked 4C_1 hexopyranoses. The potential energy surfaces exhibit roughly three distinct regions: the main domain, containing the A and B wells, which encompasses more than half of the energetically stable conformations, and two separated regions, named C and D (containing the D, E wells for N-G). The major structural features of the minima of the different A, B, C, D, E wells are summarized in Tables I and II for G-N and N-G, respectively. For all the minima, the hydroxymethyl group of the N residue presents the GT orientation, which is generally the most represented one in solution for glucose and glucose-derived sugars (Marchessault and

Table I. Energy minima of the potential energy surfaces of the disaccharide GN

Well GN	A	B	C	D
Φ_{1-3} (°)	-79.7	-91.4	-91.8	56.3
Ψ_{1-3} (°)	111.6	81.1	-69.2	128.8
γ (°)	127.3	127.4	126.8	126.2
δ (°)	136.5	144.4	87.6	96.6
ΔE (kcal/mol)	0	0.28	1.88	3.38
H bond (Å)	O ₃ (G)...O ₄ (N) 2.72	O ₅ (G)...O ₄ (N) 2.70	–	–

Pérez, 1979). The general behavior of both disaccharides is similar with respect to their respective conformational space. The minima of A and B regions, which are extended conformations with optimal exo-anomeric effects, are very close in energy. The minimum of the C well is less than 2 kcal/mol higher in energy; this weak energy difference compared with the conformations of the main region A-B, in addition to an energy barrier less than 7 kcal/mol between the two domains, suggests the contribution of conformations from the C region in solution. The D well is isolated from the main region and contains conformations significantly higher in energy, especially for the (1→4) linked N-G disaccharide. Such a well is not likely to be populated in solution.

Intrinsic viscosity measurements have indicated that, in aqueous salt solutions, sodium hyaluronate behaves as a semi-rigid polymer (Morris *et al.*, 1980). This stiffness has been proposed to arise partly from the presence of an extended network of intramolecular hydrogen bonds (Atkins *et al.*, 1980). A first type of H bonds (2 per trisaccharide) involving the ring oxygen atoms is commonly accepted. Both the slow periodate oxidation of the glucuronic residue (G) in HA (Scott and Tigwell, 1978) and the dramatic decrease of the dimensions in highly alkaline solutions strongly suggest their occurrence.

In contrast, the hydrogen bonds involving the acetamido group are still debated. The *trans* orientation of this group established in water by NMR (Cowman *et al.*, 1984; Sicinska *et al.*, 1993) is incompatible with the direct hydrogen bond between the NH (N) and COO⁻ (G) groups, originally proposed by Atkins and coworkers (Atkins *et al.*, 1980). In the present study, the results of the conformational search performed on the disaccharides indicate that the conformations of the lowest A, B energy regions are stabilized by the presence of the hydrogen bonds involving the ring oxygen atoms (see Tables I, II). In contrast, none of the two hydrogen bonds involving the acetamido group were observed. This exocyclic

group invariably adopted the stable *trans* orientation. As mentioned previously, dimers are too short to provide pertinent information about the structural parameters contributing to the stiffness of HA, the favored conformations of the two trisaccharides N-G-N and G-N-G were investigated further. Only the conformations arising from the combination of the low energy conformers of each disaccharide component were considered. The fully optimized structures were those maintaining the conformational features which were observed in the disaccharides. Thus, at the trisaccharide level, a network of hydrogen bonds, involving the contiguous ring oxygens, clearly appeared (Figure 3); the acetamido group did not participate in this network as it never forms any hydrogen bond with OH or COOH group of the adjacent residue. Nevertheless, for all the trimers generated, the distance between amide proton and the carboxylate oxygen of the N-G component is compatible with the inclusion of only one bridging water molecule. As another possible source of stiffening, the relative energies of the trimers (data not shown), indicated significant interaction for longer oligomers. The region D, and regions C, D, E of G-N and N-G components, respectively, became inaccessible at the trisaccharide level.

Conformational properties of HA chains

Because of the important biological functions of hyaluronan, particular interest has been focused on the hydrodynamic and rheological properties of hyaluronate solutions, especially their viscoelasticity. From several experimental studies, solution properties have been interpreted by a stiffened random coil (Cleland and Wang, 1970; Morris *et al.*, 1980). NMR (Darke *et al.*, 1975) and viscosity (Morris *et al.*, 1980) studies indicated the occurrence of ordered domains in solution. Recent investigations carried out on HA of bacterial origin led to the conclusion that the polymer is best represented as a wormlike polymer perturbed by ionic effects (Fouissac *et al.*, 1992) and characterized by an intrinsic persistence length in the range of 70–80 Å (Fouissac *et al.*, 1992).

Theoretically, configurational characteristics can be calculated from statistical samples of disordered chains using molecular mechanics. In the present study, the disordered chains were generated for different temperatures, from the energetic data of the disaccharide and tetrasaccharide segments, using the corresponding (Φ, Ψ) energy maps. The usual approach consists of using the (E, Φ, Ψ) triads referring to the disaccharide subunits and thus, the calculated dimensions refer to the unperturbed state of the polymer, experimentally observed in the θ -conditions. Using this procedure, a persistence length of 55 Å is predicted, which represents a value below the recent experimental ones

Table II. Energy minima of the potential energy surfaces of the disaccharide NG

Well NG	A	B	C	D	E
Φ_{1-4} (°)	-90.9	-70.1	-98.3	52.1	73.5
Ψ_{1-4} (°)	-169.6	-120.1	54.1	-120.3	-92.1
γ (°)	6.3	0.2	115.9	-8.3	-97.5
δ (°)	139.9	131.4	139.1	153.9	140.5
ΔE (kcal/mol)	0	0.22	0.06	5.20	5.52
H bond (Å)	O ₅ (N)...O ₃ (G) 2.70	O ₅ (N)...O ₃ (G) 2.85	O ₅ (N)...O ₃ (G) 2.96	–	–

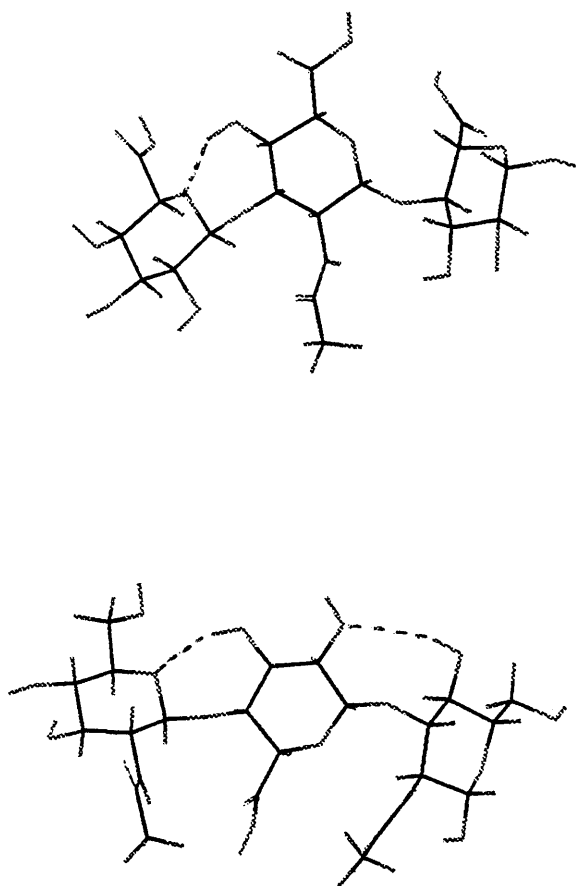
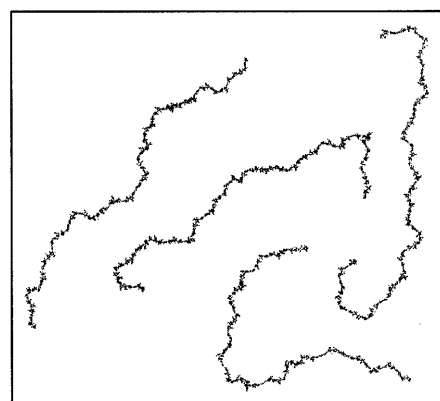


Fig. 3. Lowest energy conformers of the trisaccharides G-N-G and N-G-N showing the hydrogen bonds involving the ring oxygens and connecting the consecutive residues.

(Rinaudo *et al.*, 1999). One considers that some longer range interactions between sugar units are not completely taken into account when the disaccharide unit is used; so, calculations were performed in a second step using the energy maps corresponding to the central N-G and G-N glycosidic linkages of the G-N-G-N and N-G-N-G tetrasaccharides, respectively. In these conditions, a value of 75 Å is calculated for the persistence length at 25°C using a dielectric constant of 80; this value characterizes a semi-rigid polymer with moderate extension. This value agrees well with the experimental one and confirms the presence of significant interaction between sugar units in larger oligomers. Snapshots of typical polymer conformations are presented in Figure 4a, illustrating the moderately extended and sinuous character of HA chains. The variations of the persistence length (L_p vs. x) at different temperatures are shown in Figure 4b. Asymptotic behavior was reached for values of about 500 glycosyl residues at 298 K. It corresponds to a characteristic ratio of about 22. Increasing the temperature regularly decreases L_p and C_∞ , but Figure 4b indicates a moderate effect of the temperature on these parameters. Despite the intrinsic limitations of the theoretical calculations (lack of water, counterions, problems arising from excluded volume effects), the agreement obtained between theoretical and experimental values, in θ -conditions, suggests that the conformational behavior of the polysaccharide chain may be properly simulated using reasonable approximations.

a)



b)

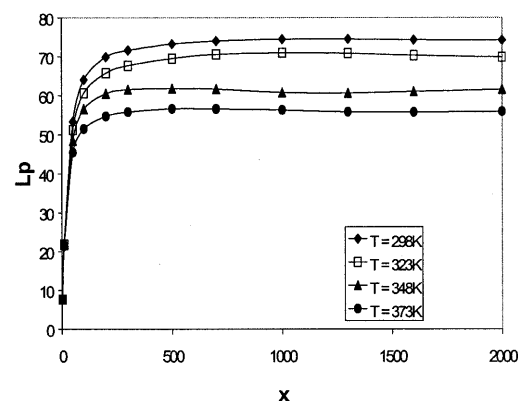


Fig. 4. (a) Snapshot of the disordered chains of HA at 25°C. (b) Persistence length, L_p (Å), calculated as a function of the number of glycosyl residues, x , of the HA chain and varying with temperature. The values are averaged over a statistical sample of 20,000 polymer chains generated using the (E, Φ , Ψ) triad data of the tetrasaccharide fragments N-G-N-G and G-N-G-N.

The ordered chain conformations

From the combination of minima of both N-G and G-N potential energy surfaces, HA oligomers exhibiting regular helical conformations have been extrapolated and minimized. Considering the oligomerization effects observed on the trisaccharides (see above), only the minima from the A, B, C regions for G-N and from the A-B region for N-G were used. The structural and energetic parameters of the helices generated are reported in Table III. Side and top views of the corresponding structures are given in Figure 5.

The main result arising from the data in Table III is that HA polysaccharide can assume a wide range of energetically stable integral helices, ranging from the left handed 4-fold symmetry

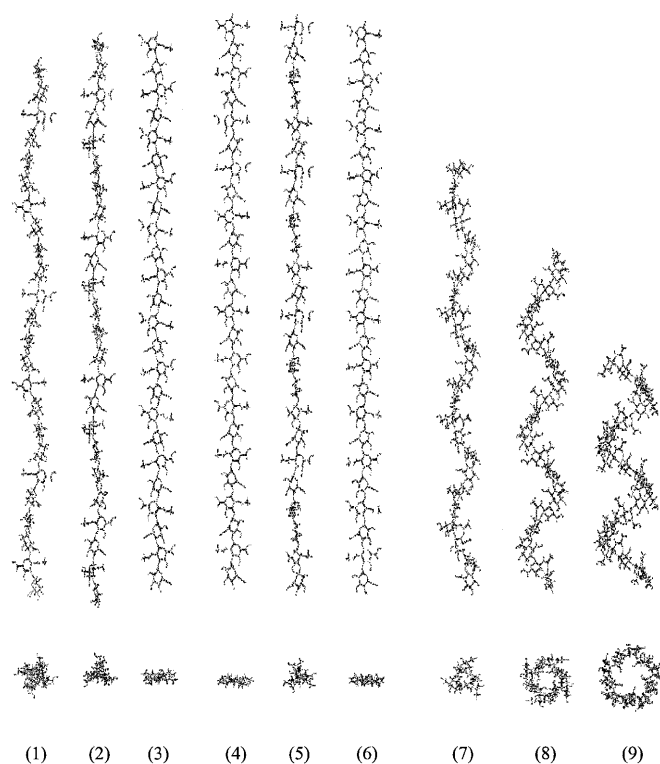


Fig. 5. Stable regular helical conformations of single strand of HA chains. The helices are represented using projection parallel and orthogonal to their axes.

Table III. Structural and energetic parameters of the stable single strand helical conformations of hyaluronan

helix	(1)	(2)	(3)	(4)	(5)	(6)	(7)	(8)	(9)
n	-4	-3	2	2	-3	2	3	4	5
h dim	9.5	9.8	9.9	10.0	10.0	10.1	7.4	5.9	4.0
ΔE_{dim} (kcal/mol)	0.61	0	0.66	0.90	1.15	1.64	0.65	2.12	1.88

to the right-handed 5-fold symmetry. Helical structures generated from the lowest A-B regions of both G-N and N-G disaccharide subunits have extended 4-, 3-, or 2-fold conformations with a rise per dimer, h , ranging from 9.51 to 10.13 Å. The helices constructed from the energy of the minimum C, for N-G component, are right-handed hollow helices (Figure 5: helices 7–9). It can be seen that the left-handed models are lower in energy than the corresponding right-handed models. The results indicate that small variations in glycosidic torsion angles may have a significant influence on the symmetry and pitch of the resulting helices without any noticeable energetic cost. Such variations are expected to occur through interactions of HA with counterions and water, and with variations in pH and temperature adopted for the preparation of the fibers. Consequently, important polymorphism may be expected for HA, and indeed, the three lowest theoretical helical conformations, which present a different symmetry: 2-fold helices and left-handed 3- and 4-fold helices illustrate well the versatility of HA in the solid state.

Fiber studies and refinements have effectively identified numerous allomorphs which are all left-handed 3- and 4-fold, and 2-fold helices with axial rises per disaccharide in the range of those calculated in the present study. It has been established that these helical conformations of HA strongly depend on the nature of the counterions and on the pH, and more moderately on the temperature and relative humidity (RH). Above pH 4.0, at room temperature and 80–85% RH, sodium (Sheehan and Atkins, 1983; Mitra *et al.*, 1985–1986) and potassium (Sheehan and Atkins, 1983; Mitra *et al.*, 1985–1986) hyaluronates adopted pseudo left-handed 4-fold conformations in an orthorhombic unit cell, with an axial rise per disaccharide being 8.4 and 9.0 Å, respectively. On drying or heating these samples, slight rearrangements occur; a more extended conformation is obtained on heating (70°C) Na-hyaluronate ($h = 9.3$ Å) (Sheehan and Atkins, 1983) and on drying K-hyaluronate ($h = 9.6$ Å) (Sheehan and Atkins, 1983; Mitra *et al.*, 1985–1986). A tetragonal unit cell is obtained on drying Na-HA (Guss *et al.*, 1975; Sheehan and Atkins, 1983) (0% RH) without changes in the helical parameters. Below pH 4.0, very different helical conformations are obtained, with a different effect for the two ions. In the presence of sodium (Sheehan and Atkins, 1983), the conformation of the chain is that of a two-fold helix, with an axial rise/disaccharide of 9.8 Å; this conformation is the most extended form of hyaluronate trapped in the solid state. Concerning K-HA, an antiparallel double-stranded helix is observed (Arnott *et al.*, 1983); the backbone of individual chains is a contracted left-handed 4-fold helix with an h value of 8.2 Å. This helical conformation has been debated and detailed model buildings and structure analysis have been presented for this form. The HA duplex with 4_3 symmetry was first trapped at low pH by Sheehan *et al.* (1977) in oriented polycrystalline fibers containing K^+ , NH_4^+ , Rb^+ or Cs^+ ions. These ions are known to disrupt “water structure” (Frank and Evans, 1945) and the double helical structure is a general response to their presence. The model established by the authors (abbreviated as X1) provided acceptable x-ray discrepancy indices but proposed an helical conformation of the individual chains quite different from that described by Guss *et al.* (1975) for HA single helix with the same 4_3 symmetry and comparable axial advance/disaccharide. Later, Arnott *et al.* (1983) reinvestigated the hyaluronan double helix. They proposed a crystal model (abbreviated as X2) with a mutual arrangement of the chains comparable to that of the first model, but with different helical conformation. Even if this refined model is more likely because of the helical conformation, close to that of the single helix, it is difficult to reject the first structure as both models provided comparable R factors.

The present work provides the way to explore the occurrence of double helical structures for HA. Starting from the helical structure optimized to reproduce both the experimental 4-fold left-handed chirality and axial advancement ($h = 8.2$ Å), all possible associations in double helix have been explored with respect to the relative orientation (parallel and anti-parallel) and position (rotation: μ , translation: ΔZ). The anti-parallel arrangement of the chains appeared to be significantly favorable compared to the parallel arrangement; this is in agreement with experimental data suggesting such arrangement as a result of chain folding. The calculations indicate that there is roughly only one way to associate the chains in double helix: all the viable anti-parallel duplexes differ from each other by

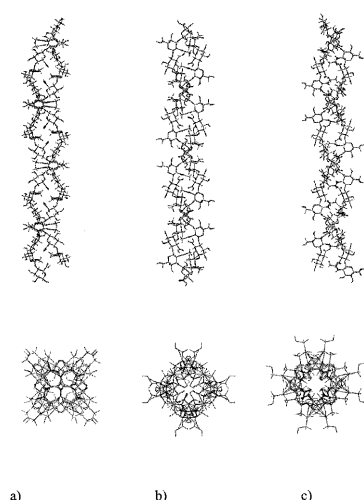


Fig. 6. Models for double helical conformations of HA with anti-parallel strands. (a) calculated model; (b) second model derived from x-ray experiment, X2, proposed by Arnott and coworkers (Arnott *et al.*, 1983); (c) first model derived from x-ray experiment, X1, proposed by Sheehan and coworkers (Sheehan *et al.*, 1977).

maximum 10° in relative rotation (μ) and $\sim 2 \text{ \AA}$ in relative translation. The geometrical and helical parameters of the best optimized duplex along with those of the two minimized x-ray models (the three models are minimized under the same conditions) are reported in Table IV, and the three models are illustrated in Figure 6. From these results, one can immediately see that the first x-ray model, X1, exhibits a very high energy, arising mainly from glycosidic torsion angles of the individual chains far from the favorable ones (see Tables I and II and Figures 2a,b). The reinvestigated x-ray model, X2, is energetically much more stable. Examination of the geometrical features of the chains indicates that the best theoretical structure and X2 model have very similar glycosidic and exocyclic (acetamido and carboxyl groups) torsion angles, with a noticeable exception for Ψ_{1-4} . We are fully aware that our modeling study provides an estimate of the internal energy of the macromolecular system rather than the free-energy, and it is this latter that determines the most favored conformations in solution. Nevertheless, the conformation of the first x-ray model is so far from the most stable ones that it can be discarded, even though the influence of the solvation and salt effects were not considered. The two x-ray models exhibit an inter-chain network of hydrophobic interactions, via the methyl groups of the acetamido moieties. X2 model exhibits an important network of intra- and inter-chain hydrogen bonds (Arnott *et al.*, 1983). Despite being absent from our theoretical calculation, this network may be very appealing. It is nevertheless questionable, as it results from a particular chain conformation with a ψ_{1-4} torsion angle 30° above a stable value (see Table II, B well) and glycosidic C-O-C valence angles (C1-O4-C4 = 118.8° [NG linkage]) which deviate from the usually observed ones.

A particular behavior of HA is observed in the presence of calcium ions (Winter and Arnott, 1977; Sheehan and Atkins, 1983). At $\text{pH} > 4$, Ca-HA crystallizes in a hexagonal unit cell and adopts a left-handed 3-fold conformation with $h = 9.5 \text{ \AA}$; this helical form is stable to changes in temperature, humidity and ionic strength. The effect of calcium is to initiate the 3-fold

Table IV. Geometrical and helical parameters of the best optimized duplex along with those of two minimized x-ray models

	a	b (X2)	c (X1)
$\Phi_{1-3}(\text{^\circ})$	-75.0	-70	-121.2
$\Psi_{1-3}(\text{^\circ})$	114.8	116.4	117.9
$\Phi_{1-4}(\text{^\circ})$	-79.2	-79.5	-120.9
$\Psi_{1-4}(\text{^\circ})$	-117.7	-89.5	118
$\Delta E(\text{kcal/mol})$	0	66.5	122.1

helix as any contamination of sodium or potassium hyaluronate by this divalent cation (even at substoichiometric levels) changes the dominant conformation to that of the 3-fold helix typical of a pure Ca-form. This particular conformational behavior related to the presence of calcium ions suggests specific interaction between HA and Ca^{2+} . Nevertheless, screening ion-chain interaction for the three helical forms, (Figure 5: helices 1 to 7) and Na^+ , K^+ , and Ca^{2+} ions using the GRID MD program (Goodford, 1985) failed to identify any specific structural features in the 3_2 conformation for calcium binding with respect to the two other forms, and did not bring a satisfying explanation concerning the behavior of HA in the presence of calcium. This procedure was successfully used in a preceding similar study realized on four polyuronides (Braccini *et al.*, 1999) known to form complex bonds with calcium in solution or gel. The lack of water in the procedure and the inherent approximation of the GRID calculations probably represent too strong limitations to get meaningful results for a system such as hyaluronate. Indeed, the fiber diffraction studies indicated that water is essential to coordinate the cations and maintain the ordered environment.

Conclusion

The present study provided a set of conformational information allowing for a better understanding of the specific behavior of hyaluronan in both solution and solid states. Important oligomerization effects have been observed in the energetic evaluation of the trisaccharides N-G-N and G-N-G. These effects reduce noticeably the accessible conformational space established on the basis of the N-G and G-N disaccharide subunits. They could represent a contribution to the inherent stiffness of hyaluronan, in addition to the network of intramolecular hydrogen bonds involving the ring oxygens. This characteristic feature of HA is also suggested by the evaluation of the dimensions of the polysaccharide: the persistence length calculated from a statistical sample of disordered chains is properly predicted, 75 \AA at 25°C , only when using (E , Φ , Ψ) data corresponding to tetrasaccharides in the procedure; it is also predicted that L_p decreases when the temperature increases.

Another characteristic feature probed in this theoretical study is the polymorphism of HA observed in the solid state. The versatility of the polysaccharide, illustrated by three different helical conformations 3_2 , 4_3 , 2_1 , is well predicted here; it is explained by weak energetic costs ($<0.7 \text{ kcal/mol-dimer}$) associated to small variations in Φ , Ψ glycosidic torsion angles leading to the different types of helix. Finally, we investigated the feasibility of a double helix with anti-parallel strands for HA, and evaluated the two models derived

from x-ray experiments. The calculations demonstrated that the formation of a duplex by chain folding is possible; though marginally observed, the anti-parallel arrangement of the chains in the double helix is more favorable than the parallel one for HA. The energetic evaluation of the x-ray models, in comparison to the established theoretical model, indicated that the first model originally proposed by Sheehan and coworkers is not viable, and that the second one proposed by Arnott *et al.* is much more reasonable, with may be an over-evaluated hydrogen bond network.

References

- Allinger, N.L., Yuh, Y.H. and Lii, J.H. (1989) Molecular mechanics. The MM3 force field for hydrocarbons. *J. Am. Chem. Soc.*, **111**, 8551–8566.
- Allinger, N.L., Rahman, M. and Lii, J.H. (1990) A molecular mechanics force field (MM3) for alcohols and ethers. *J. Am. Chem. Soc.*, **112**, 8293–8307.
- Allinger, N.L., Zhu, Z.Q.S. and Chen, K. (1992) Molecular mechanics (MM3) studies of carboxylic acids and esters. *J. Am. Chem. Soc.*, **114**, 6120–6133.
- Almond, A., Sheehan, J.K. and Brass, A. (1997) Molecular dynamics simulations of the two disaccharides of hyaluronan in aqueous solution. *Glycobiology*, **7**, 597–604.
- Arnott, S., Mitra, A.K. and Raghunathan, S. (1983) Hyaluronic acid double helix. *J. Mol. Biol.*, **169**, 861–872.
- Atkins, E.D.T., Phelps, C.F. and Sheehan, J.K. (1972) The conformation of the mucopolysaccharides; hyaluronates. *Biochem. J.*, **128**, 1255–1263.
- Atkins, E.D.T., Meader, D. and Scott, J.E. (1980) Model for hyaluronic acid incorporating four intramolecular hydrogen bonds. *Int. J. Biol. Macromol.*, **2**, 318–319.
- Boutherin, B., Mazeau, K. and Tvaroska, I. (1997) Conformational statistics of pectin substances in solution by a Metropolis Monte Carlo study. *Carbohydr. Polymers*, **31**, 1–12.
- Braccini, I., Grasso, R.P. and Pérez, S. (1999) Conformational and configurational features of acidic polysaccharides and their interactions with calcium ions: a molecular modeling investigation. *Carbohydr. Res.*, **317**, 119–130.
- Cleland, R.L. and Wang, J.L. (1970) Ionic polysaccharides. III. Dilute solution properties of hyaluronic acid fractions. *Biopolymers*, **9**, 799–810.
- Cowman, M.K., Kozart, D., Nakayashi, K. and Balazs, E.A. (1984) ¹H NMR of glycosaminoglycans and hyaluronic acid oligosaccharides in aqueous solution: the amide proton environment. *Arch. Biochem. Biophys.*, **230**, 203–212.
- Darke, A., Finer, E.G., Moorhouse, R. and Rees, D.A. (1975) Studies of hyaluronate solutions by nuclear magnetic relaxation measurements. Detection of covalently defined, stiff segments within the flexible chains. *J. Mol. Biol.*, **99**, 477–486.
- Engelsen, S.B., Cros, S., Mackie, W. and Pérez, S. (1996) A molecular builder for carbohydrates: application to polysaccharides and complex carbohydrates. *Biopolymers*, **39**, 417–433.
- Fouissac, E., Milas, M., Rinaudo, M. and Borsali, R. (1992) Influence of the ionic strength on the dimensions of sodium hyaluronate. *Macromolecules*, **25**, 5613–5617.
- Frank, H.S. and Evans, M.W. (1945) Entropy in binary liquid mixture; partial molal entropy in dilute solutions: structure and thermodynamics in aqueous electrolytes. *J. Chem. Phys.*, **13**, 507–532.
- French, A.D., Rowland, R.S. and Allinger, N.L. (1990) Computer modeling of carbohydrate molecules. *A.C.S. Symposium Series 430*. American Chemical Society, Washington, DC, 120–140.
- Goldberg, R.L. and Tolle, B.P., (1984) Pericellular coat of chick embryo chondrocytes: Structural role of hyaluronate. *J. Cell. Biol.*, **99**, 2114–2121.
- Goodford, P.J. (1985) A computational procedure for determining energetically favorable binding sites on biologically important macromolecules. *J. Med. Chem.*, **28**, 849–857.
- Guss, J.M., Hukins, D.W.L., Smith, P.J.C., Winter, W.T., Arnott, S., Moorhouse, R. and Rees, D.A. (1975) Hyaluronic acid: molecular conformations and interactions in two sodium salts. *J. Mol. Biol.*, **95**, 359–384.
- Hardingham, T. (1981) Proteoglycans; their structure, interactions and molecular organization on cartilage. *Biochem. Soc. Trans.*, **9**, 489–497.
- Hascall, V.C. (1981) Proteoglycans: structure and function. *Biol. Carbohydr.*, **1**, 1–49.
- Imberty, A., Hardman, K.D., Carver, J.P. and Pérez, S. (1991) Molecular modeling of protein-carbohydrate interactions. Docking of monosaccharides in the building site of concanavalin A. *Glycobiology*, **1**, 631–642.
- IUPAC-IUB (1983) *Joint Commission on Biochemical Nomenclature (JCBN)*. *Arch. Eur. J. Biochem.*, **131**, 5.
- Kaufmann, J., Möhle, K., Hofmann, H.J. and Arnold, K. (1998) Molecular dynamics study of hyaluronic acid in water. *J. Mol. Str. (Theochem)*, **422**, 109–121.
- Lapasin, R. and Prici, S. (1995) *Rheology of Industrial Polysaccharides, Theory and Applications*. Blackie Academic and Professional, imprint of Chapman and Hall, Glasgow, pp. 63–83.
- Laurent, T.C. (1970) The structure of hyaluronic acid. In Balazs, E.A. (ed.), *Chemistry and Molecular Biology of the Intercellular Matrix*, Vol. 2. Academic Press, New York, pp. 703–732.
- Marchessault, R.H. and Pérez, S. (1979) Conformation of the hydroxymethyl group in crystalline aldohexopyranoses. *Biopolymers*, **18**, 2369–2374.
- Metropolis, N., Rosenbluth, A.W., Rosenbluth, M.M., Teller, A.H. and Teller, E. (1953) Equation of state calculations by fast computing machines. *J. Chem. Phys.*, **21**, 1087–1092.
- Mikuni-Takagi, Y. and Toole, B.P. (1980) Cell-substratum attachment and cell surface hyaluronate of Rous sarcoma virus-transformed chondrocytes. *J. Cell Biol.*, **85**, 481–488.
- Mitra, A.K., Arnott, S., Millane, R.P., Raghunathan, S. and Sheehan, J.K. (1985–1986) Comparison of glycosaminoglycan structures induced by different monovalent cations as determined by x-ray fiber diffraction. *J. Macromol. Sci.-Phys.*, **B24 (1–4)**, 21–38.
- Morris, E.R., Rees, D.A. and Welsh, E.J. (1980) Conformation and dynamic interactions in hyaluronate solutions. *J. Mol. Biol.*, **138**, 383–400.
- Pérez, S. (1990) A priori crystal structure modeling of polymeric materials. In Fryer, J.R. and Dorset, D.L. (eds.), *Electron Crystallography of Organic Molecules*. London: Kluwer Academic, pp. 33–53.
- Pérez, S., Imberty, A. and Scaringe, R.P. (1990) Computer modeling of carbohydrate molecules. *A.C.S. Symposium Series 430*. American Chemical Society, Washington, DC, pp. 281–299.
- Rinaudo, M., Roure, J. and Milas, M. (1999) Use of steric exclusion chromatography to characterize hyaluronan, a semirigid polysaccharide. *Int. J. Polym. Anal. Charact.*, **5**, 277–287.
- Scott, J.E. and Tigwell, M. (1978) Periodate oxidation and the shapes of glycosaminoglycans in solution. *Biochem. J.*, **173**, 103–114.
- Scott, J.E., Cumming, C., Brass, A. and Chen, Y. (1991) Secondary and tertiary structures of hyaluronan in aqueous solution, investigated by rotary shadowing-electron microscopy and computer simulation. *Biochem. J.*, **274**, 699–705.
- Sheehan, J.K. and Atkins, E.D.T. (1983) X-Ray fiber diffraction study of the conformational change in hyaluronate induced in the presence of sodium, potassium and calcium cations. *Int. J. Biol. Macromol.*, **5**, 215–221.
- Sheehan, J.K., Gardner, K.H. and Atkins, E.D.T. (1977) Hyaluronic acid: a double helical structure in the presence of potassium at low pH and found also with the cations ammonium, rubidium and caesium. *J. Mol. Biol.*, **117**, 113–135.
- Sicinska, W., Adams, B. and Lerner, L. (1993) A detailed ¹H and ¹³C NMR study of a repeating disaccharide of hyaluronan: the effects of temperature and counterion type. *Carbohydr. Res.*, **242**, 29–51.
- Turley, E.A. and Roth, S., (1980) Interactions between the carbohydrate chains of hyaluronate and chondroitin sulfate. *Nature*, **283**, 268–271.
- Underhill, C.B. and Dorfman, A. (1978) The role of hyaluronic acid in intercellular adhesion of cultured mouse cells. *Exp. Cell Res.*, **117**, 155–164.
- Winter, W.T. and Arnott, S. (1977) Hyaluronic acid: the role of divalent cations in conformation and packing. *J. Mol. Biol.*, **117**, 761–784.
- Winter, W.T. and Smith, P.J.C. (1975) Hyaluronic acid: structure of a fully extended 3-fold helical sodium salt and comparison with the less extended 4-fold helical forms. *J. Mol. Biol.*, **99**, 219–235.